The Egyptian Journal of Remote Sensing and Space Sciences (2013) **16**, 11–16

National Authority for Remote Sensing and Space Sciences

The Egyptian Journal of Remote Sensing and Space Sciences

www.elsevier.com/locate/ejrs
www.sciencedirect.com

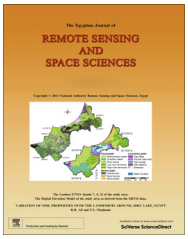

RESEARCH PAPER

Simultaneous spacecraft orbit estimation and control based on GPS measurements via extended Kalman filter

Tamer Mekky Ahmed Habib *

The Egyptian National Authority for Remote Sensing and Space Science, Cairo, Egypt

Received 9 May 2012; revised 31 October 2012; accepted 18 November 2012
Available online 21 December 2012

KEYWORDS

Orbit;
Control;
Estimation;
EKF;
GPS;
Drag;
Random disturbance

Abstract The primary aim of this work is to provide simultaneous spacecraft orbit estimation and control based on the global positioning system (GPS) measurements suitable for application to the next coming Egyptian remote sensing satellites. Disturbance resulting from earth's oblateness till the fourth order (i.e., J_4) is considered. In addition, aerodynamic drag and random disturbance effects are taken into consideration.

1. Introduction

An estimation algorithm is used frequently to provide estimates of states to the control algorithm. The estimation algorithm utilizes the provided measurements coming from different sensors to obtain the required estimates of the states. These estimates are usually obtained in a least square sense to overcome the degradation coming from various disturbance sources acting on the sensors and the plant under consideration. Extended Kalman filter could be used as a standard estimation algorithm that could deal efficiently with the nonlinearities associated with the plant (the process) and the measurement processes. The unscented Kalman filter (Bhanderi, 2005), and the derivative free implementation of the extended Kalman filters (Quine, 2006), are other forms or substitutes of the extended Kalman filter those could deal more efficiently with the high nonlinearities. Unfortunately, these substitutes of the extended Kalman filter are characterized by high computational load that may not be suitable for application onboard a spacecraft. Simple estimation and control algorithms are considered to be a must onboard any spacecraft. Thus, a control algorithm such as that given in Luo and Tang (2005) is considered to be not adequate due to its complexity. The most common approaches of orbit control existing in the literature depend on C–W equations which describe two adjacent spacecraft's relative motion as shown in Yang et al. (2010), Zhang et al. (2011). But these equations, in addition to those found in Jah and Kelecy (2010), did not include the effect of earth's oblateness, limited thrust budget, or aerodynamic drag. The algorithms found in Tamer (2011), have the advantage of simplicity in addition to being able to include the effect of earth's oblateness till the fourth order (i.e., J_4), limited thrust budget, and aerodynamic drag. The research at hand utilizes the extended Kalman filter for state estimation due to its relative low computational load compared to other estimation algorithms. In addition, the

* Tel.: +20 124207654.
E-mail address: tamermekky@hotmail.com

Peer review under responsibility of National Authority for Remote Sensing and Space Sciences.

ELSEVIER Production and hosting by Elsevier

http://dx.doi.org/10.1016/j.ejrs.2012.11.002

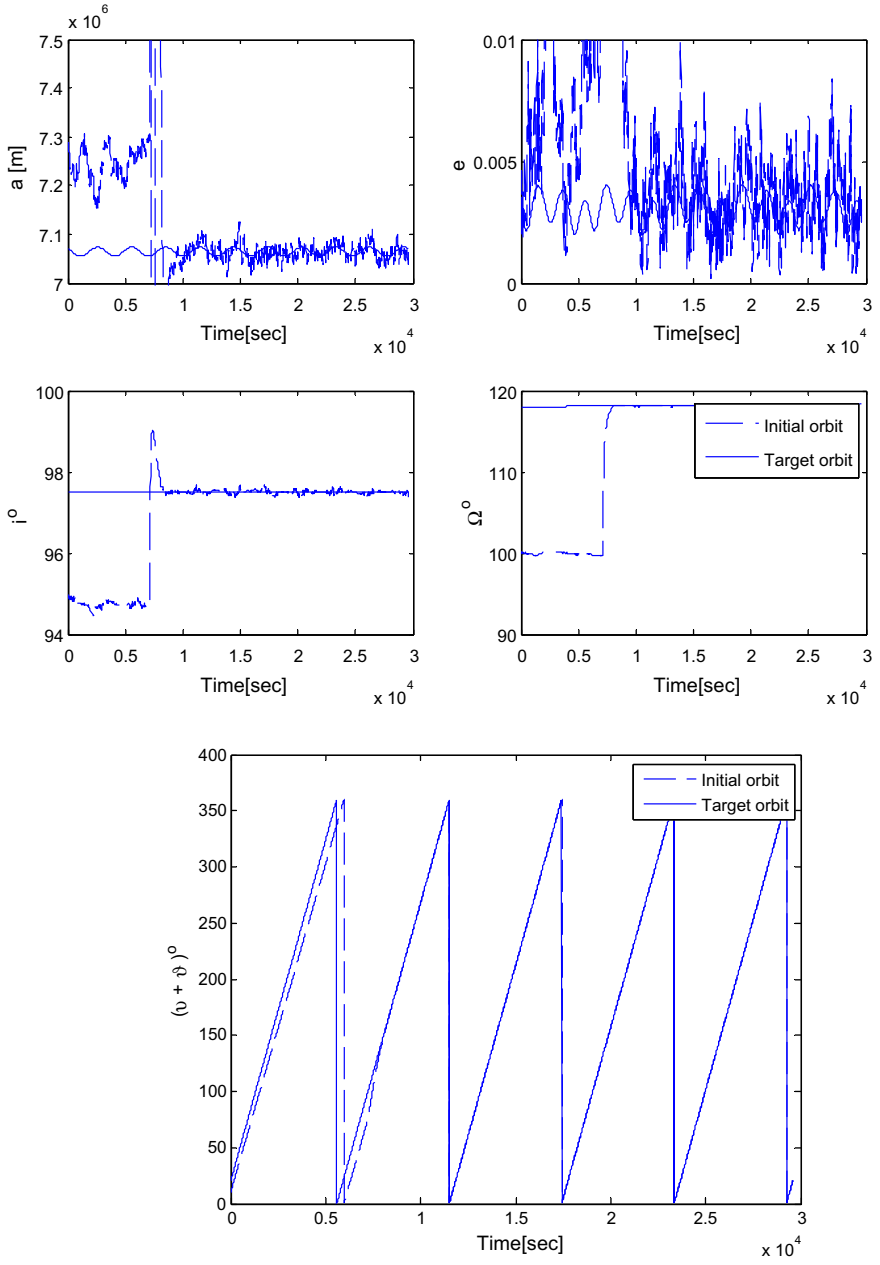

Figure 1 Orbital parameters for the initial and target orbits.

control algorithm strategy of Tamer (2011), is adopted due to the same reason. Thus, simultaneous spacecraft orbit estimation and control is achieved taking into account disturbance sources such as earth's oblateness till the fourth order (i.e., J_4), limited thrust budget, and aerodynamic drag. Simplicity of the estimation and control algorithms could also be counted as surplus essential advantages. These advantages make them suitable for application onboard the next Egyptian remote sensing satellite, when the need arise to them.

2. Modeling spacecraft orbital motion and perturbations

The spacecraft orbital motion model is essentially that is well known by Cowell's formulation (Tamer, 2009). The spacecraft orbital motion model is given as

$$\overset{o}{X} = \begin{bmatrix} \overset{o}{X}_I \\ \overset{o}{Y}_I \\ \overset{o}{Z}_I \\ \overset{oo}{X}_I \\ \overset{oo}{Y}_I \\ \overset{oo}{Z}_I \end{bmatrix} = \begin{bmatrix} 0 & 0 & 0 & 1 & 0 & 0 \\ 0 & 0 & 0 & 0 & 1 & 0 \\ 0 & 0 & 0 & 0 & 0 & 1 \\ \frac{-\mu}{\|R_I\|^3} & 0 & 0 & 0 & 0 & 0 \\ 0 & \frac{-\mu}{\|R_I\|^3} & 0 & 0 & 0 & 0 \\ 0 & 0 & \frac{-\mu}{\|R_I\|^3} & 0 & 0 & 0 \end{bmatrix} \begin{bmatrix} X_I \\ Y_I \\ Z_I \\ \overset{o}{X}_I \\ \overset{o}{Y}_I \\ \overset{o}{Z}_I \end{bmatrix} + \begin{bmatrix} 0 \\ 0 \\ 0 \\ a_{XI} \\ a_{YI} \\ a_{ZI} \end{bmatrix} = f(X) \qquad (1)$$

where R is the position vector of the spacecraft defined in the inertial axes (the subscript $_{(I)}$ denotes the inertial axes. i.e., $R_I = [X_I \quad Y_I \quad Z_I]^T$), μ_E the gravitational constant of the earth ($\mu_E = 3.986 \times 10^{14}\ \mathrm{m^3/s^2}$), $a_I = [a_{XI} \quad a_{YI} \quad a_{ZI}]^T$ the perturbing accelerations expressed in the inertial frame of reference and $\overset{o}{()}$ denotes the time derivative.

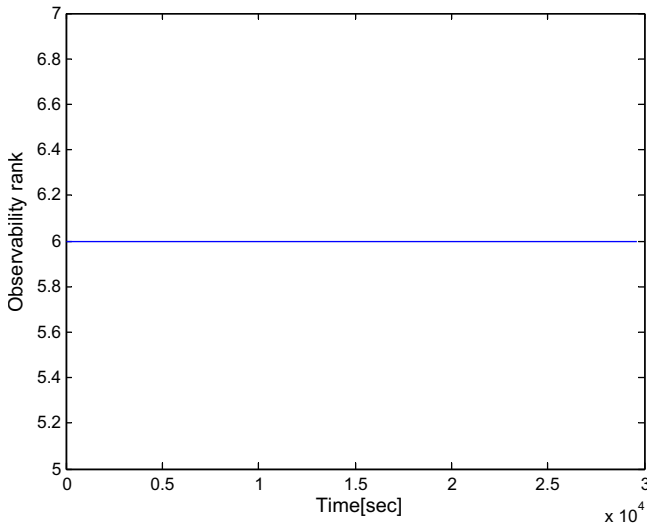

Figure 2 Rank of the observability matrix during orbital maneuver execution.

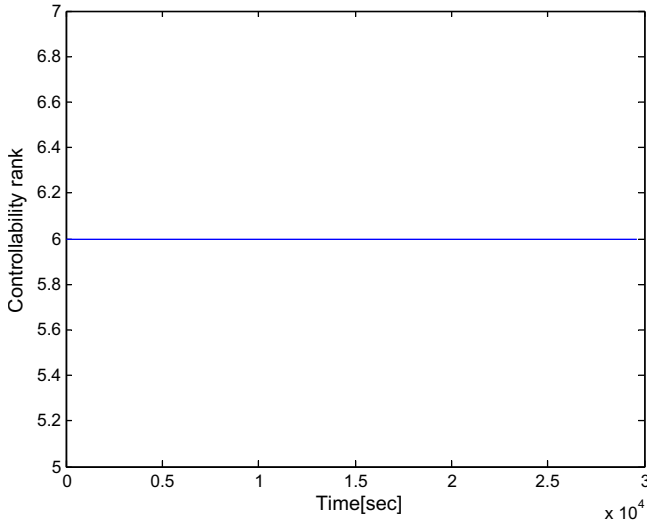

Figure 3 Rank of the controllability matrix during orbital maneuver execution.

The effect of earth's oblateness and aerodynamic drag is given as follows (Tamer, 2011).

2.1. Perturbation models

2.1.1. The earth oblateness

The gravity field affecting the motion of a spacecraft in a two-body Keplerian orbit assumes a perfectly spheroid shape of the earth. However, for higher accuracies of spacecraft position the ellipsoidal shape of the earth must be used instead. The gravitational potential function of the earth could be expanded in a spherical harmonic form as

$$U = \frac{\mu_E}{r_S}\sum_{l=0}^{l\max}\sum_{m=0}^{l}\left(\frac{R_\oplus}{r_S}\right)^l P_{lm}\{C_{lm}\cos(m\phi_S) + S_{lm}\sin(m\phi_S)\} \quad (2)$$

where $R_\oplus$ is the earth's mean equatorial radius ($R_\oplus = 6378.1363\times10^3$m), P_{lm}: are associated Legendre functions, m is the model order, l is the model degree, C_{lm}, and S_{lm} are the dimension-less coefficients used to describe the shape and mass distribution inside the earth, r_S is the geocentric distance and ϕ_S is the east longitude from Greenwich.

If the selected coordinate system in which the potential function is calculated coincides with the geocentric equatorial axes, the terms, $C_{1,0}$, $C_{1,1}$, and $S_{1,0}$ become zero. The term $C_{0,0}$ is equal to 1 and is corresponding to a spherical earth model. Thus, Eq. (2) turns out to be

$$U = \frac{\mu_E}{r_S}\left(1 + \sum_{l=2}^{l\max}\sum_{m=0}^{l}\left(\frac{R_\oplus}{r_S}\right)^l P_{lm}\{C_{lm}\cos(m\phi_S) + S_{lm}\sin(m\phi_S)\}\right) \quad (3)$$

The associated Legendre polynomial could be computed recursively by the relations (Vallado, 2001):-

$$P_{0,0} = 1 \quad (4)$$

$$P_{l,l} = (2l-1)P_{l-1,l-1}\cos\lambda \quad (5)$$

$$P_{l,0} = \frac{(2l-1)P_{l-1,0}\sin\lambda - (l-1)P_{l-2,0}}{l} \quad (6)$$

$$P_{l,m} = P_{l-2,m} + (2l-1)P_{l-1,m-1}\cos\lambda \quad (7)$$

where λ is the latitude.

The partial derivatives of the gravitational potential function are

$$\frac{\partial U}{\partial r_S} = \frac{-\mu}{r_S^2}\sum_{l=2}^{l\max}\sum_{m=0}^{l}\left(\frac{R_\oplus}{r_S}\right)^l (l+1)P_{l,m}\{C_{l,m}\cos(m\phi_S) + S_{l,m} \times \sin(m\phi_S)\} \quad (8)$$

$$\frac{\partial U}{\partial \lambda} = \frac{\mu}{r_S}\sum_{l=2}^{l\max}\sum_{m=0}^{l}\left(\frac{R_\oplus}{r_S}\right)^l \{P_{l,m+1} - m\tan(\lambda)P_{l,m}\}\{C_{l,m} \times \cos(m\phi_S) + S_{l,m}\sin(m\phi_S)\} \quad (9)$$

$$\frac{\partial U}{\partial \phi_S} = \frac{\mu}{r_S}\sum_{l=2}^{l\max}\sum_{m=0}^{l}\left(\frac{R_\oplus}{r_S}\right)^l mP_{l,m}\{S_{l,m}\cos(m\phi_S) - C_{l,m} \times \sin(m\phi_S)\} \quad (10)$$

and finally, the perturbation acceleration in the earth centered earth fixed (ECEF) coordinate system is:

$$a_{XE} = \left\{\frac{1}{r_S}\frac{\partial U}{\partial r_S} - \frac{Z_E}{r_S^2\sqrt{X_E^2+Y_E^2}}\frac{\partial U}{\partial \lambda}\right\}X_E - \frac{1}{X_E^2+Y_E^2} \times \frac{\partial U}{\partial \phi_S}Y_E \quad (11)$$

$$a_{YE} = \left\{\frac{1}{r_S}\frac{\partial U}{\partial r_S} - \frac{Z_E}{r_S^2\sqrt{X_E^2+Y_E^2}}\frac{\partial U}{\partial \lambda}\right\}Y_E - \frac{1}{X_E^2+Y_E^2} \times \frac{\partial U}{\partial \phi_S}X_E \quad (12)$$

$$a_{ZE} = \frac{1}{r_S}\frac{\partial U}{\partial r_S}Z_E + \frac{\sqrt{X_E^2+Y_E^2}}{r_S^2}\frac{\partial U}{\partial \lambda} \quad (13)$$

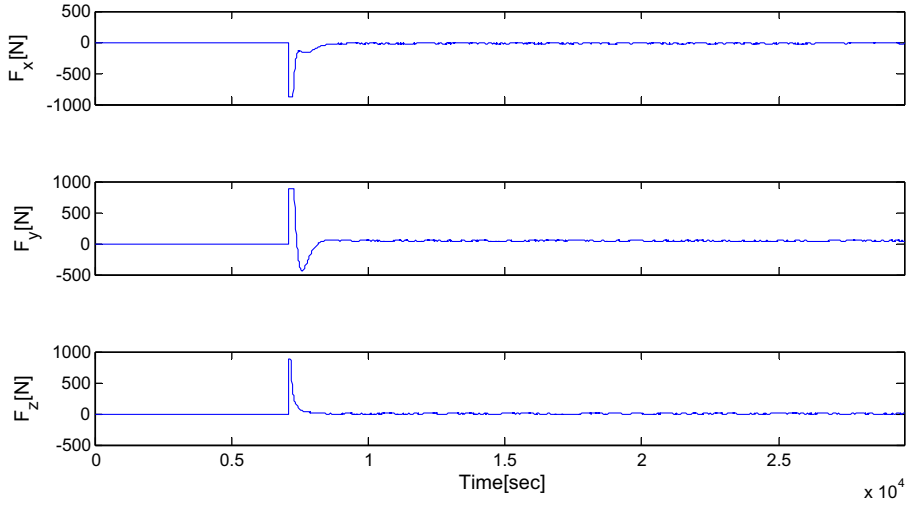

Figure 4 Time history of thrust force.

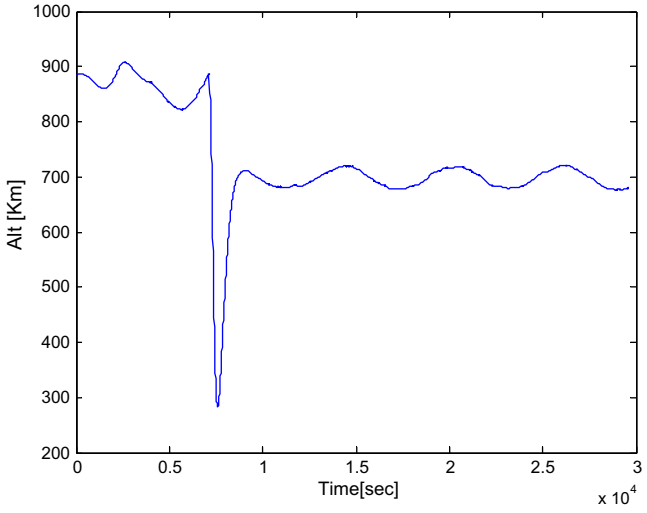

Figure 5 Satellite altitude.

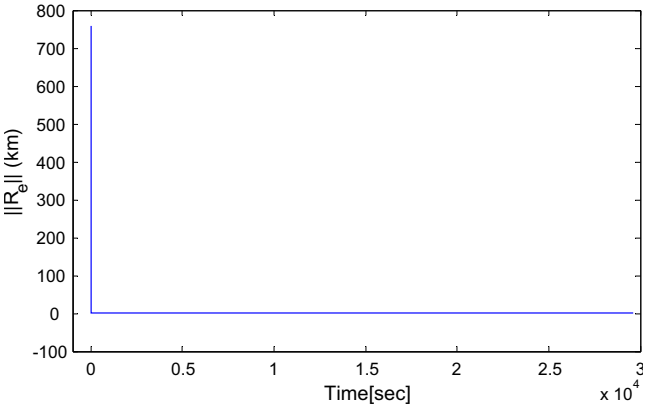

Figure 6 Satellite position estimation error.

where X_E, Y_E, and Z_E are the spacecraft position vector components in the earth centered earth fixed (ECEF) coordinate system.

The accelerations resulting from oblateness of the earth could be transformed from the ECEF frame of reference to the inertial frame (ECI) through the relation

$$\begin{bmatrix} a_{XI} \\ a_{YI} \\ a_{ZI} \end{bmatrix} = \begin{bmatrix} \cos\alpha_g & -\sin\alpha_g & 0 \\ \sin g_g & \cos\alpha_g & 0 \\ 0 & 0 & 1 \end{bmatrix} \begin{bmatrix} a_{XE} \\ a_{YE} \\ a_{ZE} \end{bmatrix} \tag{14}$$

and α_g is the Greenwich right ascension determined from Tamer (2011).

$$\alpha_g = \alpha_{g0} + 1.002737903 \times 2\pi \times D \tag{15}$$

where α_{g0} is the 1.74933340 rad at 1/1/1970 0^h:0^m:0^s and D is the time in day fraction elapsed since 1/1/1970 0^h:0^m:0^s.

2.1.2. Aerodynamic drag

The aerodynamic force, df_{Aero} on a satellite surface element dA, is given by Tamer (2011).

$$df_{Aero} = -\frac{1}{2} C_D \rho V^2 dA \tag{16}$$

where V is the translational velocity of the satellite t relative to the incident stream, ρ is the atmospheric density, and C_D is the drag coefficient. For practical applications C_D may be set in the range of 2.0.

The atmospheric density is modeled based on interpolation between the values given in Larson and Wertz (1999).

3. Spacecraft orbit control

The control laws are given by Tamer (2011)

$$a_{XIc} = k_x(X_I^{commanded} - X_{IE}) + k_{xd}(V_{xI}^{commanded} - V_{xIE}) \tag{17}$$

$$a_{YIc} = k_y(Y_I^{commanded} - Y_{IE}) + k_{yd}(V_{yI}^{commanded} - V_{yIE}) \tag{18}$$

$$a_{XIc} = k_z(Z_I^{commanded} - Z_{IE}) + k_{zd}(V_{zI}^{commanded} - V_{zIE}) \tag{19}$$

where $a_{Ic} = [\,a_{XIc} \quad a_{YIc} \quad a_{ZIc}\,]^T$ are the control accelerations provided to the spacecraft expressed in the inertial frame of reference, $[\,k_x \quad k_{xd} \quad k_y \quad k_{yd} \quad k_z \quad k_{zd}\,]^T$ are the controller

gains in the X, Y, and Z directions and $()_E$ denotes that the variable is provided by the estimator.

4. Spacecraft orbit estimation

Spacecraft orbit estimation process is done throughout the extended Kalman filter. Measurements are provided to the filter by a GPS receiver. The basic structure of the extended Kalman filter is given in Tamer (2011) as

$$\widehat{X}_k^- = f(\widehat{X}_{k-1}) \tag{20}$$

$$P_k^- = A_{k-1}P_{k-1}A_{k-1}^T + Q_{k-1} \tag{21}$$

$$K_k = P_k^- H_k^T (H_k P_k^- H_k^T + R_k)^{-1} \tag{22}$$

$$\widehat{X}_k = \widehat{X}_k^- + K_k[z_k - \hat{z}_k] \tag{23}$$

$$P_k = [I - K_k H_k]P_k^-[I - K_k H_k]^T + K_k R_k K_k^T \tag{24}$$

$$= \begin{bmatrix} 0 & 0 & 0 & 1 & 0 & 0 \\ 0 & 0 & 0 & 0 & 1 & 0 \\ 0 & 0 & 0 & 0 & 0 & 1 \\ \frac{\mu}{\|R_I\|^5}(3X_I^2 - \|R_I\|^2) & \frac{\mu}{\|R_I\|^5}(3X_I Y_I) & \frac{\mu}{\|R_I\|^5}(3X_I Z_I) & 0 & 0 & 0 \\ \frac{\mu}{\|R_I\|^5}(3X_I Y_I) & \frac{\mu}{\|R_I\|^5}(3Y_I^2 - \|R_I\|^2) & \frac{\mu}{\|R_I\|^5}(3Y_I Z_I) & 0 & 0 & 0 \\ \frac{\mu}{\|R_I\|^5}(3X_I Z_I) & (3Y_I Z_I) & \frac{\mu}{\|R_I\|^5}(3Z_I^2 - \|R_I\|^2) & 0 & 0 & 0 \end{bmatrix} \tag{27}$$

where $\hat{z}_k$ is the estimated measurement vector, z_k is the measurement vector provided by measurement devices, R_k is the discrete measurement noise covariance, Q_k is the discrete process noise covariance, P_k a posteriori estimate error covariance at a time step k, $\widehat{X}_k$ a posteriori state estimate at a time step k, $\widehat{X}_k^-$ a priori state estimate at a time step k, A_k is the state transition matrix and H_k is the measurement matrix.

The state transition matrix according to (Tamer, 2011) is calculated from

$$A_{k-1}(\widehat{X}_{k-1}^+) = \{I + (F_{k-1}(\widehat{X}_{k-1}^+))\Delta T\} \tag{25}$$

where ΔT is defined as the sampling time interval and (Tamer, 2011), (Montenbruck and Gil, 2005).

$$F_{k-1}(\widehat{X}_{k-1}^+) = \partial f/\partial X|_{\widehat{(X_{k-1}^+)}} \tag{26}$$

The measurement matrix corresponding to measurements of the GPS, H_k, is computed from

$$H_k = \begin{bmatrix} 1 & 0 & 0 & 0 & 0 & 0 \\ 0 & 1 & 0 & 0 & 0 & 0 \\ 0 & 0 & 1 & 0 & 0 & 0 \end{bmatrix} \tag{28}$$

5. Controllability and observability analysis

Controllability analysis is based mainly on the two matrices F_k and G where the matrix, G, is given by

$$G = \begin{bmatrix} 0 & 0 & 0 \\ 0 & 0 & 0 \\ 0 & 0 & 0 \\ 1 & 0 & 0 \\ 0 & 1 & 0 \\ 0 & 0 & 1 \end{bmatrix} \tag{29}$$

The controllability matrix is computed from the relation

$$CO = \begin{bmatrix} G & F_k G & F_k^2 G & F_k^3 G & F_k^4 G & F_k^5 G \end{bmatrix} \tag{30}$$

The controllability matrix given in Eq. (30) must have a full rank (i.e., 6).

Similarly, the observability matrix, OB, defined in Eq. (31) must have a rank of 6.

$$OB = \begin{bmatrix} H_k \\ H_k F_k \\ H_k F_k^2 \\ H_k F_k^3 \\ H_k F_k^4 \\ H_k F_k^5 \end{bmatrix} \tag{31}$$

6. Simulation case study and testing

The initial orbital parameters are chosen exactly as those found in Tamer (2011). The estimator initial conditions are: a (semi major axis) = 73,71,200 m, e (orbit eccentricity) = 0.002, i (orbit inclination) = 98°, Ω (right ascension of ascending node) = 102°, ϑ (argument of perigee) = 0°, and υ (true anomaly) = 16°. Fig. 1 displays the behavior of the classical orbital elements of the satellite over 30,000 s. As shown in Fig. 1, the satellite had successfully completed its orbital maneuver after about 10,000 s.

Fig. 2 represents the rank of the observability matrix defined earlier. And Fig. 3 shows the rank of the controllability. The rank of both of the matrices is equal to six which indicate a full rank. Fig. 4 displays the required thrust force for execution of the orbital maneuver. As clear in this figure, the

maximum thrust level is 890 N in all directions. The spacecraft mass under consideration is 50 kg. As clear from Fig. 4, in the beginning of the orbital maneuver, thrusters went into saturation. During the saturation period the rank of the controllability matrix is six, indicating full controllability during the saturation period. The rank of the controllability matrix will not be the only indicator for existence of control as the control channel might exist but the required control value is not available. To alleviate this difficulty, global optimum values of the controller gains are selected (taking into account the maximum available thrust force) using real coded genetic algorithms (RCGA) found in Tamer (2011). The system is designed (using RCGA) to have a time constant of 213.4516 s and a damping ratio of 0.9621. Fig. 5 represents the satellite altitude which is used only to check that the satellite did not hit the earth surface during the execution of the orbital maneuver. Fig. 6 shows the satellite position estimation error. The quick convergence of the error (typically within 10 s) from about 760 to about 0.5 km indicates the success of the estimation process. Note that, the sinusoidal behavior of the semi-major axis and the altitude is due to oblateness of the earth, as mentioned in Section 2. We should note that a successful orbital maneuver is achieved after approximately less than 500 s.

7. Conclusion

The orbit estimation and orbit control processes had worked successfully with each other. The orbit estimation algorithm provided state estimates of the spacecraft position and velocity to the orbit control algorithm. The extended Kalman filter showed a fast convergence of the estimation error. Nonlinearities of the actual spacecraft behavior resulted from aerodynamic drag, earth oblateness, and bounded thrust budget are taken into consideration during the controller design process. The rank of the controllability and observability matrices indicated a full rank. This means that the plant is fully controllable and observable. The resulting control and estimation algorithms are characterized by simplicity, which is considered to be a surplus advantage that enables their execution onboard the spacecraft computer.

References

Bhanderi, D., 2005. Spacecraft Attitude Determination with Earth Albedo Corrected Sun sensor Measurements, Ph.D. Thesis, Department of Control Engineering, Aalborg University.

Jah, M., Kelecy, T., 2010. Detection and orbit determination of a satellite executing low thrust maneuvers. Acta Astronautica 66, 798–809.

Larson, W., Wertz, J.R., 1999. Space Mission Analysis and Design. Microcosm Press, and Kluwer Academic Publisher.

Luo, Y., Tang, G., 2005. Spacecraft optimal rendezvous controller design using simulated annealing. Aerospace Science and Technology 9, 732–737.

Montenbruck, O., Gil, E., 2005. Satellite Orbits Models, Methods, Applications, third ed. Springer.

Vallado, D., 2004. Fundamentals of Astrodynamics and Applications, second ed. Microcosm Press and Kluwer Academic Publishers.

Quine, B., 2006. A derivative-free implementation of the extended Kalman filter. Automatica 24, 1927–1934.

Tamer, M., 2009. New Algorithms of Nonlinear Spacecraft Attitude Control via Attitude, Angular Velocity, and Orbit Estimation Based on the Earth's Magnetic Field, Ph.D. Thesis, Cairo University.

Tamer, M., 2011. Fast converging with high accuracy estimates of satellite attitude and orbit based on magnetometer augmented with gyro, star sensor and GPS via extended Kalman filter. The Egyptian Journal of Remote Sensing and Space Sciences 14 (2), 57–61.

Tamer, M., 2011. Global optimum spacecraft orbit control subject to bounded thrust in presence of nonlinear and random disturbances in a low earth orbit. The Egyptian Journal of Remote Sensing and Space Sciences. http://dx.doi.org/10.1016/j. ejrs.2011.08.002.

Yang, X., Gao, H., Shi, P., 2010. Robust orbital transfer for low earth orbit spacecraft with small-thrust. Journal of The Franklin Institute 347 (10), 1863–1887.

Zhang, J., Tang, G., Luo, Y., Li, H., 2011. Orbital rendezvous mission planning using mixed integer nonlinear programming. Acta Astronautica 68 (7–8), 1070–1078.